Strategic Solvent System Tuning for the Development of PVDF and TPU Nanofibers

Ömer Faruk Ünsal[a] and Ayşe Çelik Bedeloğlu[a],*

[a]Department of Polymer Materials Engineering, Bursa Technical University, Eflak Str. No: 177 Yıldırım, Bursa, 16310, Turkey.

ARTICLE INFO

ABSTRACT

In this study, we have achieved the successful fabrication of polyvinylidene fluoride (PVDF) and thermoplastic polyurethane (TPU) nanofiber samples. The key element of our investigation revolved around the manipulation of solvent systems, specifically by varying the dimethyl formamide (DMF) to acetone ratio. Our primary objective was to explore the intricate interplay between the chosen solvent system and the resultant fiber morphology. To accomplish this, we employed a multifaceted approach, which encompassed the utilization of scanning electron microscopy (SEM) to provide a comprehensive visual representation of the nanofiber structures and dimensional measurements to quantify their physical attributes. Furthermore, fourier-transform infrared (FT-IR) spectroscopy was employed to delve into the molecular-level alterations induced by the solvent systems on the macromolecular morphology of the polymer nanofibers. This systematic examination not only contributes to a deeper understanding of the nanofiber fabrication process but also holds significant potential for various applications in the realm of materials science and nanotechnology.

I. INTRODUCTION

Polymer nanofibers stand out as a prominent category of polymeric nanomaterials, primarily due to their inherent advantages, notably simplicity and cost-effectiveness. These materials, characterized by their straightforward production processes and economical nature, also exhibit exceptional characteristics attributed to their nano-scale web-like structure, encompassing attributes such as a high surface area, porosity, and low density [1, 2]. These inherent features render nanofibers as highly viable candidates for a diverse range of research endeavors. Furthermore, polymeric nanofibers lend themselves to functionalization through appropriate physical and/or chemical techniques, allowing for the customization of their properties to meet specific requirements [3–5]. Researchers have harnessed these attributes in various domains, with prevalent applications encompassing gas and liquid phase filtration [6–8], drug-delivery systems [9–11], tissue engineering [12, 13], sensors [14–16], and energy-related applications (e.g., nanogenerators, capacitors) [17, 18].

While a wide array of fabrication methods is employed for nanofiber production, including techniques such as centrifugal spinning, melt blowing, phase separation, template synthesis, and self-assembly, electrospinning reigns as the most prevalent approach [19]. Electrospinning can be fundamentally described as the process through which a polymer, in either a molten or solution state, moves from a feeding nozzle to a collector substrate under the influence of an electrical field. The application of a specific voltage magnitude (typically up to 100 kV) between the nozzle and the collector generates the requisite electrical field [20]. In essence, the polymer is propelled from the nozzle to the collector by electrostatic forces. Initially, the fluidic polymer forms a conical droplet. In the

*Corresponding author. Tel.: +90-224-300-3491; e-mail: ayse.bedeloglu@btu.edu.tr

subsequent step, this conical droplet transforms into an elongated and thin jet [21]. Beyond the foundational electrospinning process, adjustments to the fabrication setup can be made to manipulate the resulting fiber morphology. These modifications can involve alterations to the geometry of various components, such as the nozzle or collector, as well as the introduction of additional physical forces, such as magnetic fields or gas pressure [22]. Furthermore, fine-tuning fabrication parameters, which represents a simpler approach than modifying the device itself, can also be considered as a means to achieve nanofibers with the desired morphology.

The electrospinning process involves several key parameters that play pivotal roles in obtaining nanofibers with the desired morphology. These critical factors include spinning distance, applied voltage, solution parameters (comprising viscosity, concentration, polymer molecular weight, and conductivity), feeding rate, and the solvent system [23]. Spinning distance assumes importance for two primary reasons. Firstly, it directly determines the magnitude of the electrical field, as it represents the applied voltage per unit distance. In other words, increasing the spinning distance reduces the electrical field magnitude, which in turn influences the formation of the polymer jet. Secondly, the spinning distance influences the vaporization of the solvent, a crucial step in solidifying the polymer into a fibrous geometry. Increasing the spinning distance allows for more extended solvent vaporization time as the polymer jet traverses the gap between the two electrodes [24]. Applied voltage, being directly linked to the magnitude of electrical field, represents another key parameter. The applied voltage profoundly impacts the magnitude of the electrical field, thereby affecting the formation of the polymer jet [23]. Solution parameters, including viscosity, concentration, and polymer molecular weight, are interconnected factors. Concentration and molecular weight significantly affect solution viscosity, with higher polymer concentrations or larger macromolecules resulting in elevated solution viscosity [23, 25]. Excessively high or low solution viscosities are undesirable, as very low viscosity can lead to bead formation in the nanofibrous structure, while highly viscous solutions tend to produce thicker fibers during electrospinning [21]. Solution conductivity is another property which alters the resulting nanofiber morphology. Increased electrical conductivity in a polymer solution amplifies charge transfer, making the effect of the electrical field force more pronounced during fiber formation [26]. As another key parameter, feeding an excessive amount of polymer solution, implying a higher load of solvent and polymer onto the collector, can lead to an increase in nanofiber diameter or, in extreme cases, hinder fiber formation due to inadequate solvent vaporization [27].

The solvent system, which is defined as a single solvent or mixture of different solvents, in the solution holds substantial significance for nanofiber production. Indeed, the solvent system employed in the electrospinning process exerts a comprehensive influence on all the solution properties previously discussed. Typically, polymer solutions in electrospinning are formulated using at least two solvents, with one of them being highly volatile to help in the rapid solidification of the polymer jet. On the other hand, the solubility of polymers can vary from one solvent to another, which in turn alters the viscosity of the polymer solution. Different solvents may have varying degrees of affinity for a particular polymer, resulting in differences in solubility and ultimately affecting the solution's viscosity. Moreover, the electrical conductivity of the polymer solution can be modulated by the selection of different solvent systems. This variability in electrical conductivity is an important parameter in the electrospinning process, as it directly influences the response of the solution to the applied electrical field. The judicious selection of solvents is, therefore, a fundamental aspect of optimizing the electrospinning process for specific applications [28–30].

Dimethylformamide (DMF), dimethylsulfoxide (DMSO), dimethylacetamide (DMAc), and N-methyl-2-pyrrolidone (NMP) are petroleum-derived, polar, and low-volatile solvents. These solvents exhibit high dissolving power owing to their polarity, making them effective for dissolving most traditional synthetic polymers, including polyvinylidene fluoride (PVDF), polyacrylonitrile (PAN), thermoplastic polyurethane (TPU), acrylonitrile-butadiene-styrene (ABS), polystyrene (PS), among others [31–35]. As discussed in the preceding paragraph, the electrospinning process employing a solvent mixture is a well-established method for producing high-quality nanofibers. In this context, this group of solvents serves as a common low-volatile component in electrospinning processes. Notably, they are frequently identified as primary solvents for synthetic polymers in the literature. Essentially, the low-volatile constituents of solvent systems possess the capability to fully dissolve polymers. Conversely, a group of high-volatile solvents, such as tetrahydrofuran (THF), acetone, methyl-ethyl ketone (MEK), and dichloromethane (DCM), are commonly used as volatile components in electrospinning solutions [36–41]. Within this classification of high-volatile and low-volatile solvents, the DMF-acetone mixture stands out as one of the most commonly employed solvent systems for the fabrication of TPU and PVDF nanofibers. This preference is attributed to its low cost and excellent solvability properties [42–47].

In a study focused on solvent system optimization [32], the influence of the DMF/acetone ratio on nanofiber morphology was investigated. The findings indicate that an increasing acetone ratio leads to lower viscosity, a factor primarily contributing to bead formation. While this may be considered a defect, the rapid solidification of polymer jets during the electrospinning process at a high acetone ratio enhances the β-crystalline phase fraction. A similar work [48], employed a formic acid/chloroform mixture to explore its impact on the morphology of nanofibrous mats. Due to the low molecular weight of the polymer (26 kDa), electrospun nanofibers could not achieve a polymer concentration below 30% by weight in pure chloroform. The addition of the low-volatile component (formic acid) into the solvent system facilitated the production of nanofibers at concentrations below 30% polymer, with an observed trend of thinner fibers as the formic acid amount increased. Notably, a study in 2007 by Tang et al. [49], revealed a relationship between fiber thickness and solidification time. The study elucidated that polymer jets are stretched between the tip and collector until they lose their solvent completely during electrospinning. The presence of a high-volatile solvent reduces the solidification time, preventing further thinning of the jets through stretching. Conversely, an increased ratio of low-volatile solvent results in fused fibers due to prolonged evaporation time on the collector surface [50]. In summary, during the solution optimization phase, achieving a balance between high-volatile and low-volatile solvents is crucial for each polymer, even for different grades of a specific polymer.

PVDF and TPU are commonly paired polymers in advanced materials research due to their complementary characteristics. For instance, PVDF is a ferroelectric material in its beta crystalline phase but possesses limited mechanical properties, such as low elongation at the breaking point. In contrast, TPU exhibits unique elastomeric properties attributed to the presence of hard and soft segments in its molecular backbone. Therefore, the hybridization of PVDF and TPU polymers through various methods, such as blending [51–54] or hybrid electrospinning [55,56], presents a viable solution to address the mechanical limitations associated with PVDF. In this regard, the concept of nanofibrous mats based on PVDF and TPU has gained popularity. Hybridizing these two polymers in solution form can be achieved through the blending of TPU and PVDF solutions or by employing a simultaneous electrospinning process where TPU and PVDF polymers. Consequently, solvent system optimization of these PVDF and TPU polymers for electrospinning process plays a critical role to achieve the

desired material properties in hybridized nanofibrous mats. In this work, effect of the solvent system on nanofiber morphology have been investigated in detail. Specifically, the effect of the mixture ratio of acetone and dimethylformamide (DMF) mixture based solvent system, which serves as a mutual solvent for both PVDF and TPU, has been demonstrated.

II. EXPERIMENTAL METHOD

The polymers and solvents used in this study were procured as follows: TPU (130 kDa, Ravathane®, Ravago, Turkey), PVDF (350 kDa, Alfa Aesar, Germany), DMF (Merck, Saudi Arabia), and acetone (Sigma-Aldrich). The electrospinning process was carried out separately for TPU and PVDF solutions, with the following parameters: an applied voltage of 26 kV, a spinning distance of 175 mm, a solution feeding rate of 1 mL/h, and a solution concentration of 10.0% by weight. To demonstrate the influence of the solvent system on the electrospinning process, the DMF:Acetone ratio was varied. Specifically, solvent systems with different compositions were prepared, containing 35.0%, 37.5%, 40.0%, 42.5%, 45.0%, and 50.0% by weight of DMF, as outlined in Table 1.

**Table 1.** Solvent system description of PVDF and TPU nanofiber samples

Polymer	DMF % (by weight)	Acetone % (by weight)	Sample Name
PVDF	35.0	65.0	P1
PVDF	37.5	62.5	P2
PVDF	40.0	60.0	P3
PVDF	42.5	57.5	P4
PVDF	45.0	55.0	P5
PVDF	50.0	50.0	P6
TPU	35.0	65.0	T1
TPU	37.5	62.5	T2
TPU	40.0	60.0	T3
TPU	42.5	57.5	T4
TPU	45.0	55.0	T5
TPU	50.0	50.0	T6

Nanofibrous mats were imaged by scanning electron microscopy (SEM, Carl Zeiss Gemini 300) and both nanofiber diameters and number of formed beads were measured by IMAGEJ software. Fourier-Transform Infrared Spectroscopy (FT-IR) measurements were performed to show the change in macromolecular conformation of nanofibers by varying solvent systems.

III. RESULTS AND DISCUSSIONS

3.1. SEM Results

Scanning Electron Microscopy (SEM) was employed to analyze TPU and PVDF nanofibers, focusing on the quantification of bead occurrences within the nanofibrous mats and the diameters of the nanofibers. The summary of these results is presented in Figure 1. Figures 1a depicts the mean diameters of samples T1-T6 and P1-P6. It is evident that TPU nanofibers, under constant electrospinning parameters and solvent systems, exhibited notably thinner characteristics compared to PVDF nanofibers. Furthermore, the error bars displayed a higher degree of diameter uniformity in TPU nanofibers, as they remained confined within a narrower range. Additionally, both mean diameter and error bars exhibited a decreasing trend as the DMF (Dimethylformamide) concentration in the
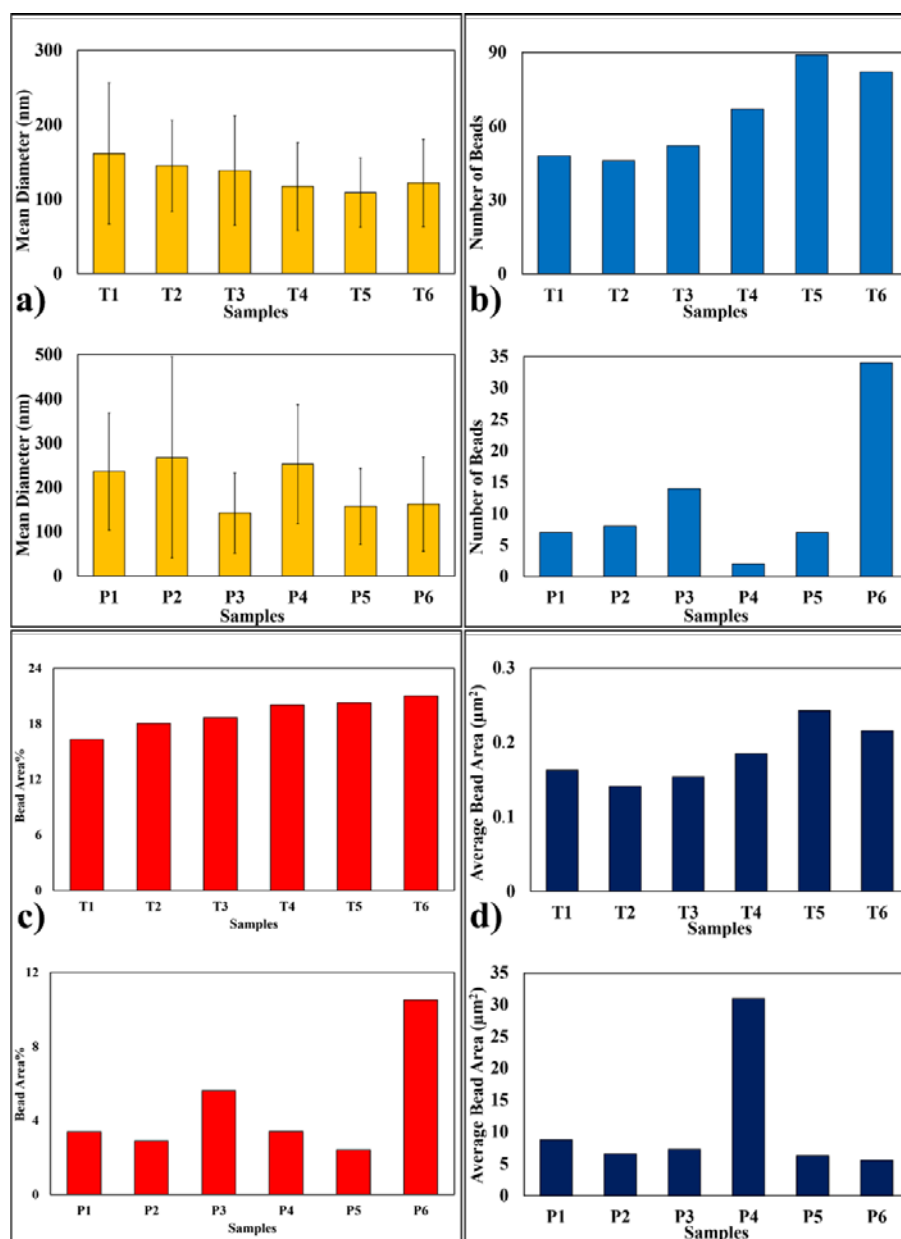
Figure 1. SEM study summarization of TPU and PVDF nanofibers; a) nanofiber diameter measurements of T1-T6 and P1-P6samples, b) bead numbers results of T1-T6 and P1-P6 samples, c) bead area percentage of T1-T6 and P1-P6 samples, and d) average bead area results of T1-T6 and P1-P6 samples

solvent system increased, up to T5. Examining Figure 1b, it becomes apparent that the diameter sizes and standard deviation ranges of PVDF nanofibers remained independent of the solvent system. On the other hand, bead formation emerged as another critical parameter for assessing the quality of nanofiber mats. Figures 1b presents the quantified number of beads in TPU and PVDF nanofibrous mats. Notably, while the number of bead formation in PVDF based nanofiber samples ranged from 2 to 34, this range expanded to 46 to 89 for TPU nanofibrous mats. This significant difference in bead formation can be directly attributed to the polymer's molecular weight and the formation of polymer atoms. Furthermore, it was observed that an increased DMF ratio led to a substantial enhancement in bead formation, a consequence of its direct influence on both viscosity and solvent volatility. Moreover, an inversely proportional relationship between fiber diameter and bead formation was particularly

notable in T5, T6, P3, and P6 samples. These four samples exhibited the highest bead counts, along with thinner diameters compared to other samples within their respective polymer groups. Conversely, P2 sample in Figure 1b appeared to be the least uniform, as it displayed only seven beads, as per SEM images.

The bead area ratio in the samples was determined to demonstrate the bead formation characteristics of TPU and PVDF polymers (Figure 1c). Total bead area in SEM images was measured using IMAGEJ software. Analysis of bead ratios in nanofibrous samples revealed that beads occupied an area ranging from 16% to 21% along TPU nanofibrous samples. In contrast, the area covered by formed beads in PVDF samples ranged from 2% to 10%. Moreover, consistent with the observation that the fiber diameter of PVDF nanofibers was bigger than that of TPU nanofibers, the average area of beads was significantly higher in PVDF samples compared to TPU samples. Besides that, average area of single beads ranged from 5 μ^2 to 30 μ^2 for PVDF mats, whereas it was between 0.14 μ^2 and 0.24 μ^2 for TPU samples. In summary, although TPU beads were smaller than PVDF beads, the presence of bead formation defects was a more pronounced issue for TPU nanofibrous mats due to a higher number of beads. Additionally, both molecular weight effect and increased DMF ratio effect on bead formation as mentioned in relevant literature [32,48] clearly seen as the result of SEM image based measurements. Similarly, reduction on fiber diameter by increasing low-volatile solvent ratio is a phenomena that matching the relevant literature [48,49].

Figure 2 and Figure 3 depict SEM images and the fiber diameter distribution graphs of TPU and PVDF-based nanofibers, respectively. The SEM images revealed that an increase in DMF concentration within the system resulted in the formation of a structure comprising half film and half fiber on the collector, impeding solvent vaporization. According to this theory, due to insufficient solvent loss during the jet's trajectory towards the collector, a buildup of the polymer solution layer occurred on the collector. Consequently, the jets reaching the collector lost their cylindrical shape, resulting in the formation of a filmic bottom side and fibrous top side structure (Figure 3f). This failed structure can also be seen as the "fused fiber problem" in the literature [50].
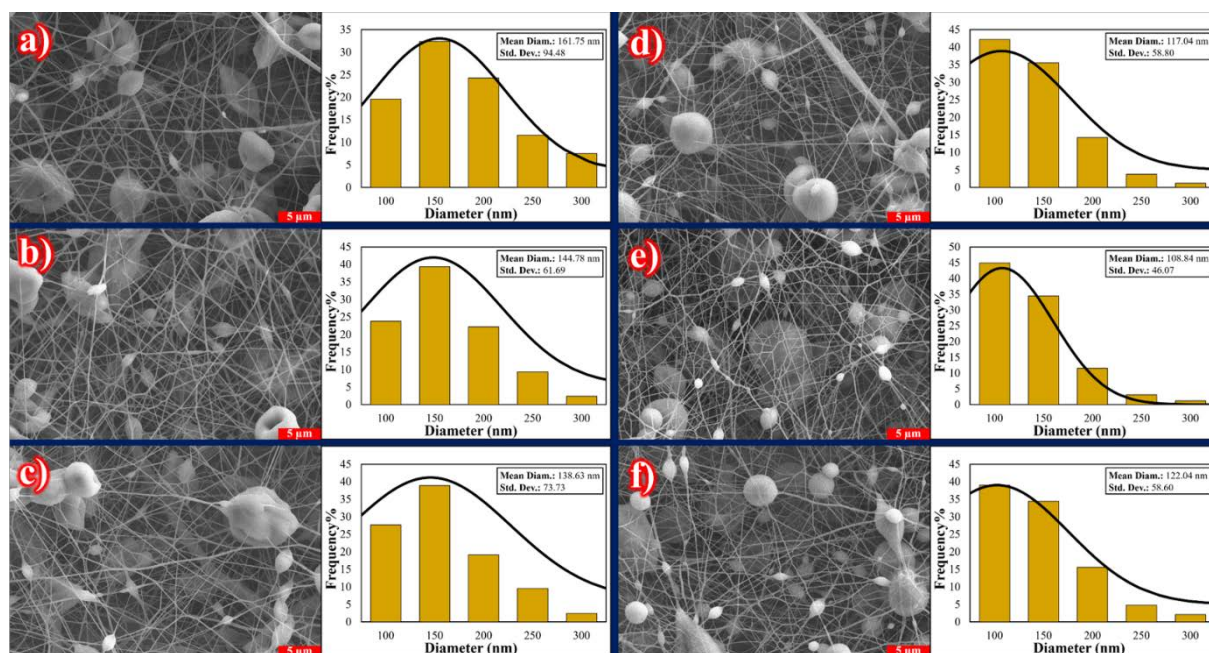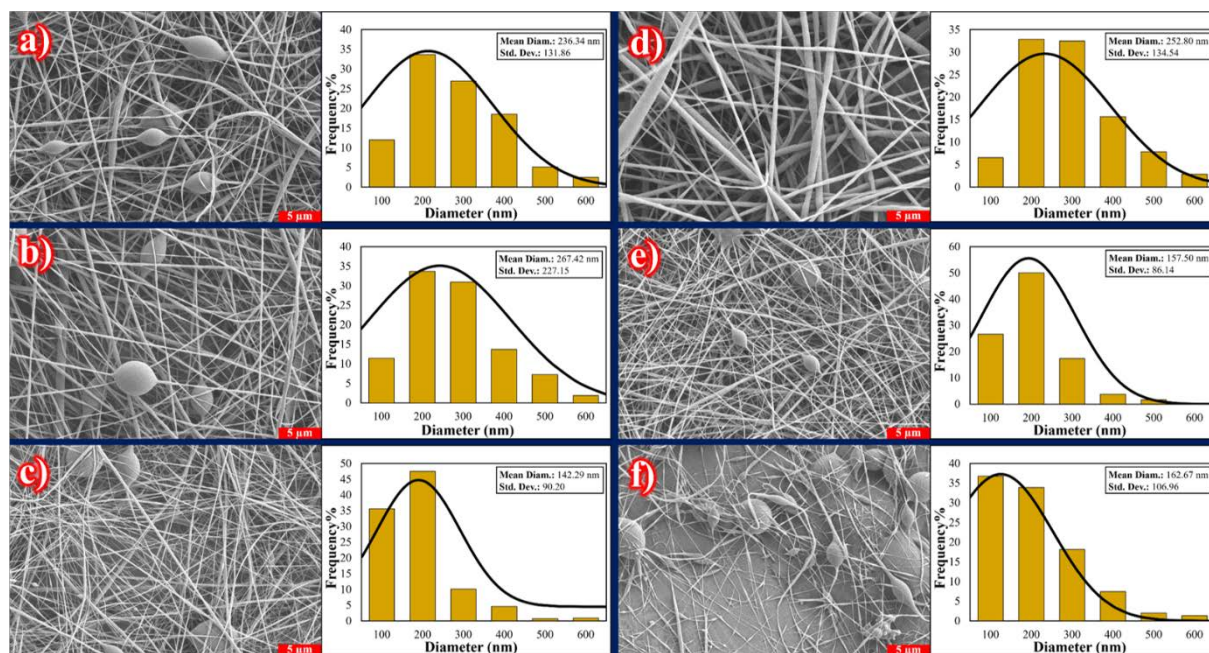

Figure 2. SEM images and diameter distribution graphs of a) T1, b) T2, c) T3, d) T4, e) T5, and f) T6

Figure 3. SEM images and diameter distribution graphs of a) P1, b) P2, c) P3, d) P4, e) P5, and f) P6

3.2. FT-IR Studies

The electrospinning process serves not only as a method for the production of nanomaterials, offering advantages of innovation, simplicity, and cost-effectiveness, but it also exerts a direct influence on macromolecular morphology, including crystallinity and crystalline phases [55,57–59]. Figure 4 presents the FT-IR results of TPU-based nanofibers. Characteristic vibrational peaks associated with TPU polymer were observed at 1219 cm^{-1} (C-N stretching), 1130-1190 cm^{-1} (C-O-C stretching), 1527 cm^{-1} (N-H bending), 1595 cm^{-1} (C=C aromatic vibration), and 1705 cm^{-1} (C=O stretching), in accordance with previous literature [60–62]. Interestingly, our findings indicate that neither the electrospinning process nor the solvent system induced significant changes in the chain morphology of TPU, a result consistent with the findings of Li's study [60].

In contrast, extensive results have been observed on the macromolecular conformation of PVDF polymer. The influence of the electrical field on PVDF chains is a well-documented phenomenon. For example, the spontaneous formation of the β-crystalline phase of PVDF during the electrospinning process enables the fabrication of electroactive nanofibrous mats. This phenomenon accounts for the prevalence of PVDF nanofiber-based piezoelectric nanogenerators [18,55]. Characteristic peaks associated with the α-crystalline phase of PVDF were

observed at 612 cm^{-1}, 762 cm^{-1}, 796 cm^{-1}, 974 cm^{-1}, 1148 cm^{-1}, and 1382 cm^{-1} (Figure 5a). Relationship between the solvent system and α-crystalline phase formation were demonstrated by zooming in on these points in Figure 5b-f. The peak intensities at these points decreased due to the electrospinning process, as the β-crystalline phase peaks increased. On the other hand, However, the intensity of the α-crystalline phase peak increased with an elevated DMF ratio in the solvent system. Similarly, the peaks associated with the formation of the β-crystalline phase (840 cm^{-1} and 1272 cm^{-1} [63,64]) during the electrospinning process at lower DMF ratios exhibited a decrease in peak intensity with increasing DMF ratio (Figure 5g-h). In other words, reducing the volatility of the solvent system results in the predominance of the α-crystalline phase in the nanofiber samples, in agreement with existing literature [65].
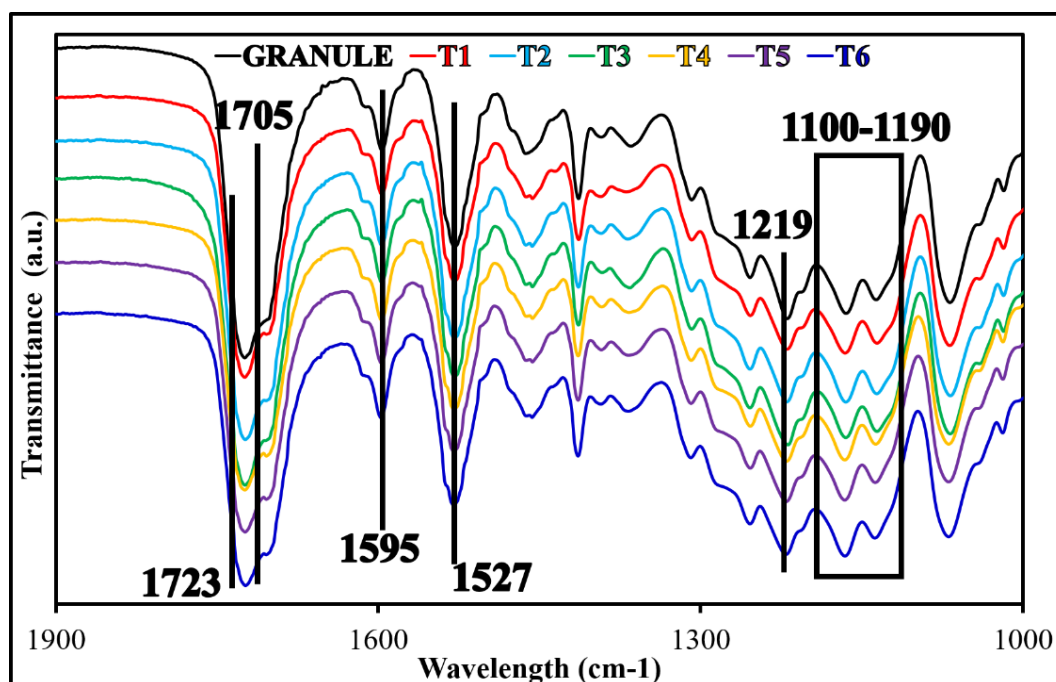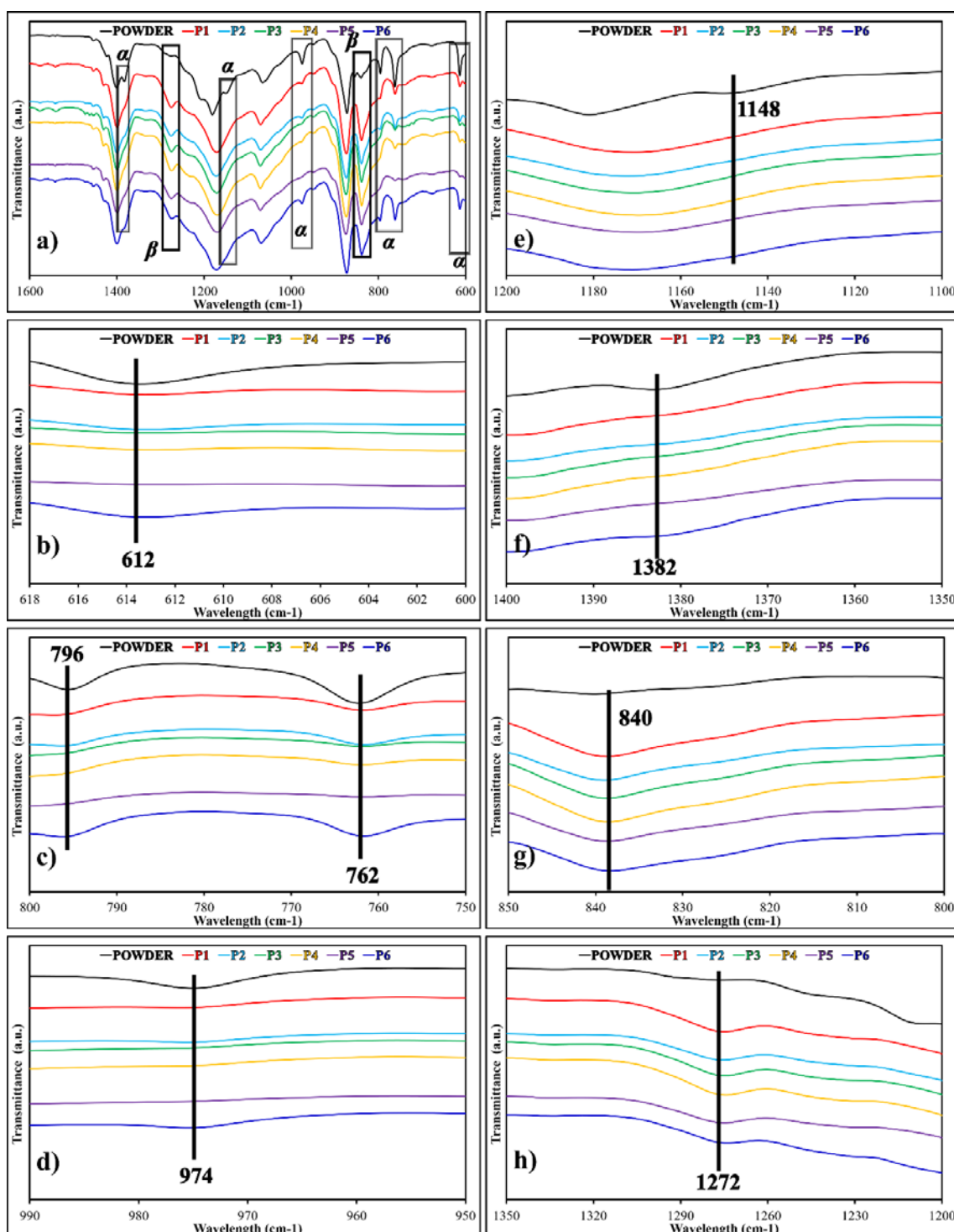

Figure 4. FT-IR spectra of TPU samples

Figure 5. a) FT-IR spectra of PVDF samples; b), c), d), e), and f) Zoomed-in spectras focusing on specific points associated with the α-crystalline phase; g) and h) Zoomed-in spectra highlighting points related to the β-crystalline phase

IV. CONCLUSIONS

Our findings reveal a direct correlation between the solvent system and fiber diameter for TPU, whereby an increased DMF ratio resulted in thinner nanofibers. Intriguingly, an increase in DMF content also led to increased

bead formation in the nanofibrous mats. In contrast, the diameter values of PVDF nanofibers, which were thicker than those of TPU nanofibers, showed no significant dependence on the solvent system. Similar to TPU nanofibers, the elevation of DMF ratio resulted in increased bead formation. Furthermore, this increase in DMF ratio led to reduced solvent volatility, resulting in a half-filmic, half-fibrous structure observed in T5, T6, P5, and P6 samples. FT-IR analysis revealed that while the solvent system had no discernible influence on the macromolecular conformation of TPU polymer during the electrospinning process, it played a pivotal role in inducing crystalline phase transitions in PVDF polymer. This study provides valuable insights into the intricate interplay between solvent systems and the resulting morphological and structural characteristics of nanofibers, enhancing our understanding of the electrospinning process and its applications.

ACKNOWLEDGMENT

REFERENCES

[1] Yun KM, Suryamas AB, Iskandar F, Bao L, Niinuma H, Okuyama K (2010) Morphology optimization of polymer nanofiber for applications in aerosol particle filtration. Separation and Purification Technology, 75, 340–345. http://doi:10.1016/j.seppur.2010.09.002

[2] Kenry, Lim CT (2017) Nanofiber technology: current status and emerging developments. Progress in Polymer Science, 70, 1–17. http://doi:10.1016/j.progpolymsci.2017.03.002

[3] Chen H, Huang M, Liu Y, Meng L, Ma M (2020) Functionalized electrospun nanofiber membranes for water treatment: A review. Science of the Total Environment, 739, 139944. http://doi:10.1016/j.scitotenv.2020.139944.

[4] Wang P, Wang Y, Tong L (2013) Functionalized polymer nanofibers: A versatile platform for manipulating light at the nanoscale. Light: Science and Applications, 2. http://doi:10.1038/lsa.2013.58

[5] Klein KL, Melechko AV, McKnight TE, Retterer ST, Rack PD, Fowlkes JD, Joy DC, Simpson ML (2008) Surface characterization and functionalization of carbon nanofibers. Journal of Applied Physics, 103 http://doi:10.1063/1.2840049

[6] Qin XH, Wang SY (2006) Filtration properties of electrospinning nanofibers. Journal of Applied Polymer Science, 102, 1285–1290. http://doi:10.1002/app.24361

[7] Zhang Q, Welch J, Park H, Wu CY, Sigmund W, Marijnissen JCM (2010) Improvement in nanofiber filtration by multiple thin layers of nanofiber mats. Journal of Aerosol Science, 41, 230–236. http://doi:10.1016/J.JAEROSCI.2009.10.001

[8] Sundarrajan S, Tan KL, Lim SH, Ramakrishna S (2014) Electrospun nanofibers for air filtration applications. Procedia Engineering, 75, 159–163. http://doi:10.1016/j.proeng.2013.11.034

[9] Zhu LF, Zheng Y, Fan J, Yao Y, Ahmad Z, Chang MW (2019) A novel core-shell nanofiber drug delivery system intended for the synergistic treatment of melanoma. European Journal of Pharmaceutical Sciences, 137, 105002. http://doi:10.1016/j.ejps.2019.105002

[10] Deepak A, Goyal AK, Rath G (2018) Nanofiber in transmucosal drug delivery. Journal of Drug Delivery Science and Technology, 43, 379–387. http://doi:10.1016/j.jddst.2017.11.008

[11] Goyal, R, Macri LK, Kaplan HM, Kohn J (2016) Nanoparticles and nanofibers for topical drug delivery. Journal of Controlled Release, 240, 77–92. http://doi:10.1016/j.jconrel.2015.10.049

[12] Barnes CP, Sell SA, Boland ED, Simpson DG, Bowlin GL (2007) Nanofiber technology: Designing the next generation of tissue engineering scaffolds. Advanced Drug Delivery Reviews, 59, 1413–1433. http://doi:10.1016/j.addr.2007.04.022

[13] Yoshimoto H, Shin YM, Terai H, Vacanti JP (2003) A biodegradable nanofiber scaffold by electrospinning and its potential for bone tissue engineering. Biomaterials, 24, 2077–2082. http://doi:10.1016/S0142-9612(02)00635-X

[14] Zhang L, Lou J, Tong L (2011) Micro/nanofiber optical sensors. Photonic Sensors, 1, 31–42.

http://doi:10.1007/s13320-010-0022-z

[15] Aussawasathien D, Dong JH, Dai L (2005) Electrospun polymer nanofiber sensors. Synthetic Metals, 154, 37–40. http://doi:10.1016/j.synthmet.2005.07.018

[16] Virji S, Huang J, Kaner RB, Weiller BH (2004) Polyaniline nanofiber gas sensors: Examination of response mechanisms. Nano Letters, 4, 491–496. http://doi:10.1021/nl035122e

[17] ALTIN Y, BEDELOĞLU A (2020) Polyacrylonitrile Nanofiber Optimization as Precursor of Carbon Nanofibers for Supercapacitors. Journal of Innovative Science and Engineering (JISE), 4, 69–83. http://doi:10.38088/jise.726792

[18] Ünsal ÖF, Altın Y, Çelik Bedeloğlu A (2020) Poly(vinylidene fluoride) nanofiber-based piezoelectric nanogenerators using reduced graphene oxide/polyaniline. Journal of Applied Polymer Science, 137, 1–14. http://doi:10.1002/app.48517

[19] Zhang X, Lu Y (2014) Centrifugal spinning: An alternative approach to fabricate nanofibers at high speed and low cost. Polymer Reviews, 54, 677–701. http://doi:10.1080/15583724.2014.935858

[20] Kiyak EY, Cakmak E (2014) Nanofiber Production Methods. Electronic Journal of Textile Technologies Tekstil, 8, 49–6049.

[21] Ziabari M, Mottaghitalab V, Haghi AK (2010) A new approach for optimization of electrospun nanofiber formation process. Korean Journal of Chemical Engineering, 27, 340–354. http://doi:10.1007/s11814-009-0309-1.

[22] Alghoraibi I, Alomari S (2018) Different Methods for Nanofiber Design and Fabrication. In: Barhoum A, Bechelany M, Makhlouf A (eds) Handbook of Nanofibers. Springer, Cham. https://doi.org/10.1007/978-3-319-42789-8_11-2

[23] Ibrahim H M, Klingner A (2020) A review on electrospun polymeric nanofibers: Production parameters and potential applications. Polymer Testing, 90, 106647. http://doi:10.1016/j.polymertesting.2020.106647

[24] Homayoni H, Ravandi SAH, Valizadeh M (2009) Electrospinning of chitosan nanofibers: Processing optimization. Carbohydrate Polymers, 77, 656–661.   http://doi:10.1016/j.carbpol.2009.02.008

[25] Katti DS, Robinson KW, Ko FK, Laurencin CT (2004) Bioresorbable nanofiber-based systems for wound healing and drug delivery: Optimization of fabrication parameters. Journal of Biomedical Materials Research - Part B Applied Biomaterials, 70, 286–296. http://doi:10.1002/jbm.b.30041

[26] Angammana CJ, Jayaram SH (2011) Analysis of the effects of solution conductivity on electrospinning process and fiber morphology. IEEE Transactions on Industry Applications, 47, 1109–1117. http://doi:10.1109/TIA.2011.2127431

[27] Abbas JA, Said IA, Mohamed MA, Yasin SA, Ali ZA, Ahmed IH (2018) Electrospinning of polyethylene terephthalate (PET) nanofibers: Optimization study using taguchi design of experiment. IOP Conference Series: Materials Science and Engineering, 454. http://doi:10.1088/1757-899X/454/1/012130

[28] Yao L, Lee C, Kim J (2010) Fabrication of electrospun meta-aramid nanofibers in different solvent systems. Fibers and Polymers, 11, 1032–1040. http://doi:10.1007/s12221-010-1032-6

[29] Tan SH, Inai R, Kotaki M, Ramakrishna S (2005) Systematic parameter study for ultra-fine fiber fabrication via electrospinning process. Polymer, 46, 6128–6134. http://doi:10.1016/j.polymer.2005.05.068

[30] Yang Z, Peng H, Wang W, Liu T (2010) Crystallization behavior of poly(ε-caprolactone)/layered double hydroxide nanocomposites. Journal of Applied Polymer Science, 116, 2658–2667. http://doi:10.1002/app.

[31] Dong X, Lu D, Harris TAL, Escobar IC (2021) Polymers and solvents used in membrane fabrication: A review focusing on sustainable membrane development. Membranes, 11. http://doi:10.3390/membranes11050309.

[32] Lei T, Yu L, Wang L, Yang F, Sun D (2015) Predicting polymorphism of electrospun polyvinylidene fluoride membranes by their morphologies. Journal of Macromolecular Science, Part B: Physics, 54, 91–101. http://doi:10.1080/00222348.2014.983853

[33] Lasprilla-Botero J, Álvarez-Láinez M, Lagaron JM (2018) The influence of electrospinning parameters and solvent selection on the morphology and diameter of polyimide nanofibers. Materials Today Communications, 14, 1–9. http://doi:10.1016/j.mtcomm.2017.12.003

[34] Halaui R, Zussman E, Khalfin R, Semiat R, Cohen Y (2017) Polymeric microtubes for water filtration by co-axial electrospinning technique. Polymers for Advanced Technologies, 28, 570–582. http://doi:10.1002/pat.3794

[35] Boaretti C, Roso M, Lorenzetti A, Modesti M (2015) Synthesis and process optimization of electrospun PEEK-sulfonated nanofibers by response surface methodology. Materials, 8, 4096–4117. http://doi:10.3390/ma8074096

[36] Lei J, Yao G, Sun Z, Wang B, Yu C, Zheng S (2019) Fabrication of a novel antibacterial TPU nanofiber membrane containing Cu-loaded zeolite and its antibacterial activity toward Escherichia coli. Journal of Materials Science, 54, 11682–11693. http://doi:10.1007/s10853-019-03727-x

[37] Cui Z, Lin J, Zhan C, Wu J, Shen S, Si J, Wang Q (2020) Biomimetic composite scaffolds based on surface modification of polydopamine on ultrasonication induced cellulose nanofibrils (CNF) adsorbing onto electrospun thermoplastic polyurethane (TPU) nanofibers. Journal of Biomaterials Science, Polymer Edition, 31, 561–577. http://doi:10.1080/09205063.2019.1705534

[38] Lin L, Choi Y, Chen T, Kim H, Lee KS, Kang J, Lyu L, Gao J, Piao Y (2021) Superhydrophobic and wearable TPU based nanofiber strain sensor with outstanding sensitivity for high-quality body motion monitoring. Chemical Engineering Journal, 419, 129513. http://doi:10.1016/j.cej.2021.129513

[39] Beniwal A, Sunny (2020) Novel TPU/Fe2O3 and TPU/Fe2O3/PPy nanocomposites synthesized using electrospun nanofibers investigated for analyte sensing applications at room temperature. Sensors and Actuators, B: Chemical, 304, 127384. http://doi:10.1016/j.snb.2019.127384

[40] Avossa J, Herwig G, Toncelli C, Itel F, Rossi RM (2022) Electrospinning based on benign solvents: current definitions, implications and strategies. Green Chemistry, 24, 2347–2375. http://doi:10.1039/d1gc04252a

[41] Barick AK, Tripathy DK (2010) Effect of nanofiber on material properties of vapor-grown carbon nanofiber reinforced thermoplastic polyurethane (TPU/CNF) nanocomposites prepared by melt compounding. Composites Part A: Applied Science and Manufacturing, 41, 1471–1482. http://doi:10.1016/j.compositesa.2010.06.009

[42] Chen C, Bai Z, Cao Y, Dong M, Jiang K, Zhou Y, Tao Y, Gu S, Xu J, Yin X, Xu W (2020) Enhanced piezoelectric performance of BiCl3/PVDF nanofibers-based nanogenerators. Composites Science and Technology, 192, 108100. http://doi:10.1016/j.compscitech.2020.108100

[43] Liao Y, Wang R, Tian M, Qiu C, Fane AG (2013) Fabrication of polyvinylidene fluoride (PVDF) nanofiber membranes by electro-spinning for direct contact membrane distillation. Journal of Membrane Science, 425–426, 30–39. http://doi:10.1016/j.memsci.2012.09.023

[44] Pisarenko T, Papež N, Sobola D, Ţălu Ş, Částková K, Škarvada P, Macků R, Ščasnovič E, Kaštyl J (2022) Comprehensive Characterization of PVDF Nanofibers at Macro-and Nanolevel. Polymers, 14, 7–9. http://doi:10.3390/polym14030593.

[45] Poorvisha R, Suriyaraj SP, Thavamani P, Naidu R, Megharaj M, Bhattacharyya A, Selvakumar R (2015) Synthesis and characterisation of 3-dimensional hydroxyapatite nanostructures using a thermoplastic polyurethane nanofiber sacrificial template. RSC Advances, 5, 97773–97780. http://doi:10.1039/c5ra18593a.

[46] Si J, Deng Yi, Gong C, Cui Z, Wang Q (2023) Preparation and characterization of deacetylated cellulose acetate/thermoplastic polyurethane nanofiber membranes modified with graphene oxide for methylene blue and Cr (VI) adsorption. Polymer Engineering and Science, 63, 3891–3905. http://doi:10.1002/pen.26494.

[47] Li W, Lu L, Yan F, Palasantzas G, Loos K, Pei Y (2023) High-performance triboelectric nanogenerators based on TPU/mica nanofiber with enhanced tribo-positivity. Nano Energy, 114, 108629. http://doi:10.1016/j.nanoen.2023.108629

[48] Pavezi KJP, Rocha A, Bonafé EG, Martins AF (2020) Electrospinning-electrospraying of poly(acid lactic) solutions in binary chloroform/formic acid and chloroform/acetic acid mixtures. Journal of Molecular Liquids, 320, 114448. http://doi:10.1016/j.molliq.2020.114448

[49] Tang C, Ye S, Liu H (2007) Electrospinning of poly(styrene-co-maleic anhydride) (SMA) and water-swelling behavior of crosslinked/hydrolyzed SMA hydrogel nanofibers. Polymer, 48, 4482–4491. http://doi:10.1016/j.polymer.2007.05.041

[50] Sharma D, Satapathy BK (2022) Optimization and physical performance evaluation of electrospun nanofibrous mats of PLA, PCL and their blends. Journal of Industrial Textiles, 51, 6640S-6665S. http://doi:10.1177/1528083720944502.

[51] Yang W, Li Y, Feng L, Hou Y, Wang S, Yang B, Hu X, Zhang W, Ramakrishna S (2020) GO/Bi2S3 doped PVDF/TPU nanofiber membrane with enhanced photothermal performance. International Journal of Molecular Sciences, 21, 1–13. http://doi:10.3390/ijms21124224

[52] Le B, Omran N, Hassanin AH, Kandas I, Gamal M, Shehata N, Shyha I (2023) Flexible piezoelectric PVDF/TPU nanofibrous membranes produced by solution blow spinning. Journal of Materials Research and Technology, 24, 5032–5041. http://doi:10.1016/j.jmrt.2023.04.051

[53] Elnabawy E, Hassanain AH, Shehata N, Popelka A, Nair R, Yousef S, Kandas I (2019) Piezoelastic PVDF/TPU nanofibrous composite membrane: Fabrication and characterization. Polymers, 11. http://doi:10.3390/polym11101634

[54] Adeli B, Gharehaghaji AA, Jeddi AAA (2021) A feasibility study on production and optimization of PVDF/PU polyblend nanofiber layers using expert design analysis. Iranian Polymer Journal (English Edition), 30, 535–545. http://doi:10.1007/s13726-021-00910-3

[55] Ünsal ÖF, Çelik Bedeloğlu A (2023) Nanofiber mat-based highly compact piezoelectric-triboelectric hybrid nanogenerators. Express Polymer Letters, 17, 564–579.

[56] Ünsal ÖF, Çelik Bedeloğlu A (2023) Three-Dimensional Piezoelectric-Triboelectric Hybrid Nanogenerators for Mechanical Energy Harvesting. ACS Applied Nano Materials, 6(16), 14656-14668. http://doi:10.1021/acsanm.3c01973

[57] Nguyen NQ, Chen TF, Lo CT (2021) Confined crystallization and chain conformational change in electrospun poly(ethylene oxide) nanofibers. Polymer Journal, 53, 895–905. http://doi:10.1038/s41428-021-00492-0

[58] El-Hadi AM, Mohan SD, Davis FJ, Mitchell GR (2014) Enhancing the crystallization and orientation of electrospinning poly (lactic acid) (PLLA) by combining with additives. Journal of Polymer Research, 21. http://doi:10.1007/s10965-014-0605-2

[59] Stephens JS, Chase DB, Rabolt JF (2004) Effect of the electrospinning process on polymer crystallization chain conformation in nylon-6 and nylon-12. Macromolecules, 37, 877–881. http://doi:10.1021/ma0351569

[60] Li B, Liu Y, Wei S, Huang Y, Yang S, Xue Y, Xuan H, Yuan H (2020) A solvent system involved fabricating electrospun polyurethane nanofibers for biomedical applications. Polymers, 12, 1–12. http://doi:10.3390/polym12123038

[61] Arik N, Horzum N, Truong YB (2022) Development and Characterizations of Engineered Electrospun Bio-Based Polyurethane Containing Essential Oils. Membranes, 12, 1–16. http://doi:10.3390/membranes12020209

[62] Jimenez GA, Jana SC (2009) Composites of Carbon Nanofibers and ThermoplasticPolyurethanes With Shape-Memory Properties Preparedby Chaotic Mixing. Polymer Engineerıng And Science, 49, 2020–2030. http://doi:10.1002/pen

[63] Shepelin NA, Glushenkov AM, Lussini VC, Fox PJ, Dicinoski GW, Shapter JG, Ellis AV (2019) New developments in composites, copolymer technologies and processing techniques for flexible fluoropolymer piezoelectric generators for efficient energy harvesting. Energy and Environmental Science, 12, 1143–1176. http://doi:10.1039/c8ee03006e

[64] Li J, Meng Q, Li W, Zhang Z (2011) Influence of crystalline properties on the dielectric and energy storage properties of poly(vinylidene fluoride). Journal of Applied Polymer Science, 122, 1659–1668. http://doi:10.1002/app.34020

[65] Gee S, Johnson B, Smith AL (2018) Optimizing electrospinning parameters for piezoelectric PVDF nanofiber membranes. Journal of Membrane Science, 563, 804–812. http://doi:10.1016/j.memsci.2018.06.050